Supporting Information

Whitehouse et al. 10.1073/pnas.0913058107

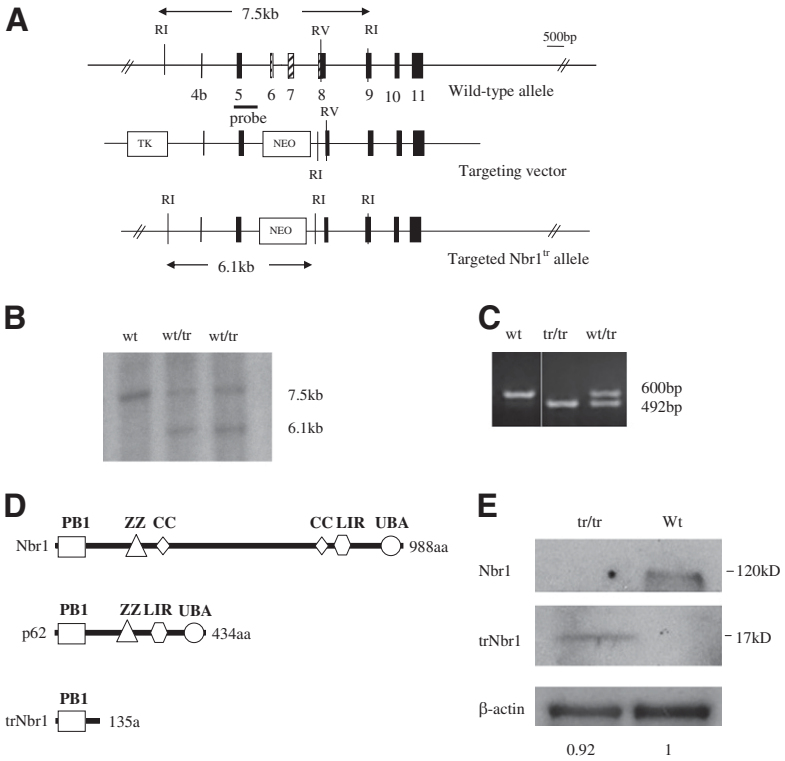

Fig. S1. Targeted disruption of neighbor of Breast cancer 1 (Brca1) gene *Nbr1*. (*A*) Schematic representation of Nbr1 targeting strategy. Boxes represent exons 4b–11 of *Nbr1*. Hashed exons are lost in the targeted allele. NEO, neomycin; TK, thymidine kinase; RI, *EcoRI*; RV, *EcoRV*. (*B*) Correct 5′ arm homologous recombination was confirmed in two embryonic stem cell clones using an exon/intron 5 probe (as shown in *A*) for Southern hybridization analysis of *EcoRI*-digested genomic DNA. (*C*) Subsequent mice were genotyped by PCR (600 bp; exon6/7 wild-type allele, 492 bp; neo). (*D*) Schematic representation of Nbr1, p62, and truncated Nbr1 (trNbr1) protein domain structure. PB1, Phox and Bem1p domain; ZZ, zinc binding; CC, coiled coil; LIR, LC3-interacting region 1; UBA, ubiquitin-associated domain. Drawn to scale. (*E*) Western blot analysis of Nbr1 and trNbr1 expression in osteoblasts from homozygous $Nbr1^{tr/tr}$ mice (tr/tr) or wild-type (Wt) mice showing ~120 kD full length and 17 kD truncated protein. Actin, loading control. Quantification of Western blots shows that both proteins are expressed at similar levels.

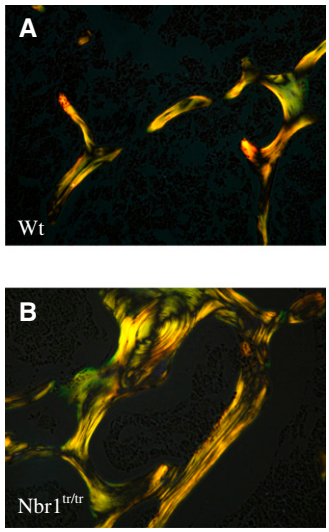

Fig. S2. Nbr1$^{tr/tr}$ bone shows properties of mature lamellar and not woven bone, as shown by parallel alignment of the collagen fibers. Histological sections of 8-mo-old (*A*) wild-type and (*B*) Nbr1$^{tr/tr}$ femurs photographed under polarized light. (Magnification: 20×.)

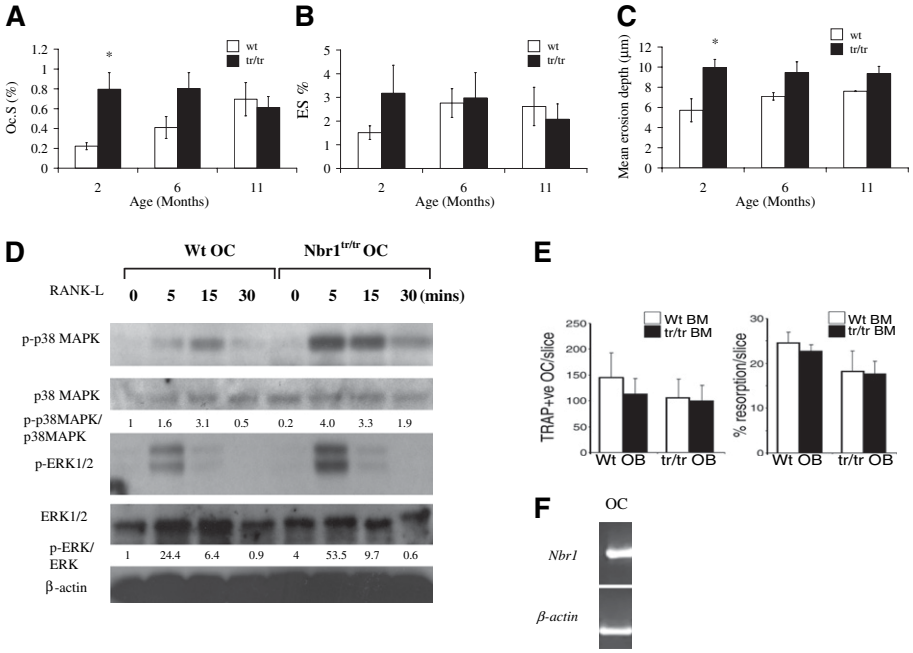

Fig. S3. Histomorphometry analysis of osteoclast parameters and cell-signaling pathway perturbation in osteoclast precursors from Nbr1$^{tr/tr}$ mice and age-matched controls. White bars, wild-type mice; black bars, Nbr1$^{tr/tr}$ mice; *x* axis, age of animals (months). (*A*) OcS, osteoclast surface. (*B*) ES, eroded surface. (*C*) Mean erosion depth. Differences between the genotypes were assessed using Student's *t* test. Error bars represent SEM ($n = 3$; $^*P < 0.05$). (*D*) Receptor activator for nuclear factor kappa B ligand (RANK-L)–induced ERK1/2 and p38 MAPK activation in isolated wild-type (Wt) and Nbr1$^{tr/tr}$ osteoclast precursor cells (OC). (*E*) Osteoclast differentiation assays. Coculture of primary calvarial osteoblasts (OBs) from WT or Nbr1$^{tr/tr}$ mice with macrophage colony stimulating factor–dependent bone marrow (BM) cells from WT or Nbr1$^{tr/tr}$ mice on dentine slices as indicated. The number of tartrate resistant acid phosphatase (TRAP) +ve osteoclasts (OC; *Left*) and percent resorption (*Right*) were quantified after 7 and 10 d, respectively. The data represent the mean ± SD of four representative dentine slices. (*F*) RT-PCR analysis confirms endogenous *Nbr1* expression in primary murine osteoclast (OC) cultures.

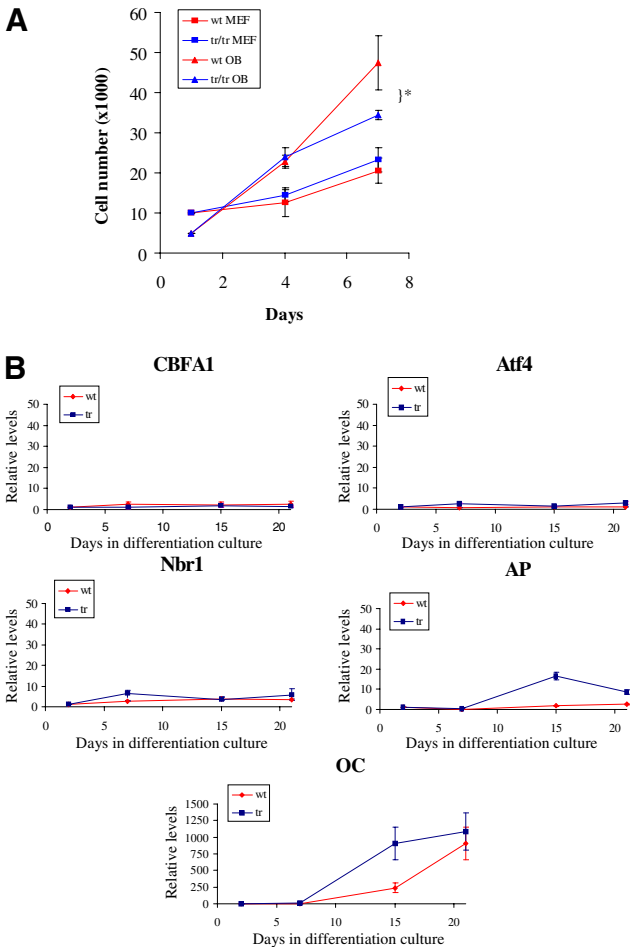

Fig. S4. (*A*) Proliferation curves for calvarial-derived osteoblasts (OB) and murine embryonic fibroblasts (MEF) from wild-type and Nbr1$^{tr/tr}$ mice. The data represents the mean ± SD of triplicate representative wells for each time point (*$P < 0.05$). (*B*) Quantitative RT-PCR analysis of OB marker gene expression in calvarial-derived osteoblast cultures from Nbr1$^{tr/tr}$ mice (blue) and Wt (red) mice during a 21-d time course of in vitro osteoblast differentiation. CBFA1/Runx2; Atf4; Nbr1; AP, alkaline phosphatase; OC, osteocalcin. Relative expression of each gene was normalized to β-actin and levels at day 2, and wild-type expression is set as 1 (*y* axis). The data represent the mean ± SD of triplicate representative wells.

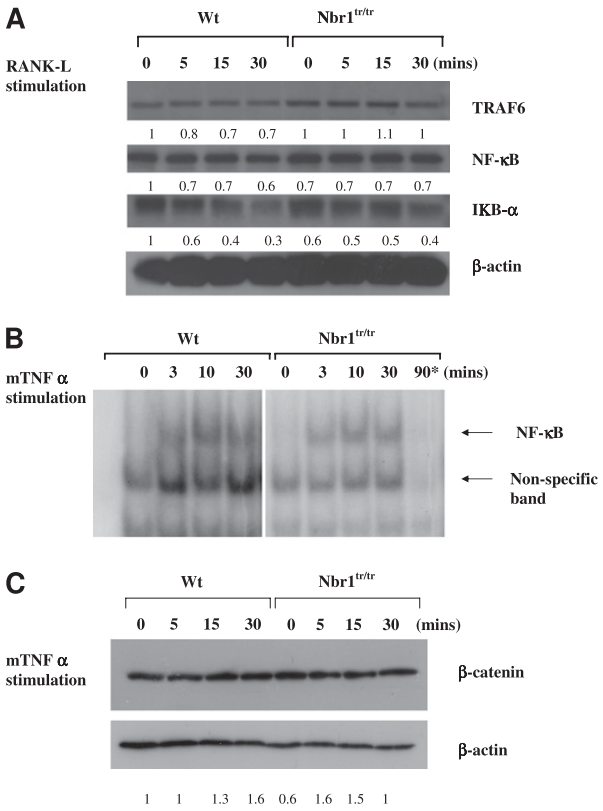

Fig. S5. Ex vivo analysis suggests that canonical Wnt and NF-κB pathways are unaffected in Nbr1$^{tr/tr}$ mice. (*A*) Western blot analysis showed no difference in levels of NF-κB pathway components after RANK-L stimulation in osteoclasts from wild-type (wt) or homozygous Nbr1$^{tr/tr}$ mice. (*B*) NF-κB mobility shift assay of nuclear extract from MEF from wild-type (wt) or homozygous Nbr1$^{tr/tr}$ mice showed no difference in TNFα-induced NF-κB nuclear accumulation. (*100-fold excess of nonradiolabeled probe shows NF-κB band specificity.) (*C*) β-catenin levels are equivalent in mTNFα-treated osteoblasts from wild-type (wt) or homozygous Nbr1$^{tr/tr}$ mice (β-actin, loading control). Quantitation shows levels of protein compared with that of untreated wild-type cells.

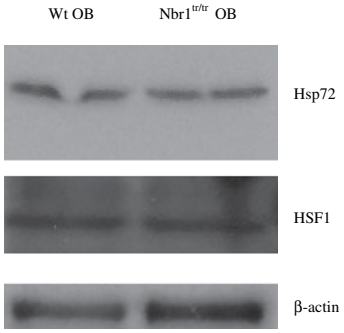

Fig. S6. Ex vivo analysis of downstream p38 MAPK effectors in osteoblasts showed no effect on protein levels by Nbr1 truncation. Wild-type (Wt) and Nbr1$^{tr/tr}$ osteoblasts (OB) were serum starved to activate the p38 MAPK pathway and analyzed for changes in levels of heat shock factor protein 1 (HSF1) and heat shock protein 72 (Hsp72). Levels are normalized to β-actin and are equivalent.

Table S1. Summary of bone mineral density (BMD) and bone-area measurements from femurs and calvariae of age-matched 3- and 9-mo-old $Nbr1^{tr/tr}$ mice and wild-type controls

	Genotype	3 mo old	*P* value	9 mo old	*P* value
Total BMD (mg/cm^3)	Wt	515.65 ± 30.08	5.59×10^{-5}	533.17 ± 77.14	2.52×10^{-5}
	tr/tr	814.44 ± 81.03		1,055.79 ± 83.41	
Trabecular BMD (mg/cm^3)	Wt	38.43 ± 24.40	2.25×10^{-4}	73.71 ± 20.42	2.07×10^{-5}
	tr/tr	416.76 ± 161.18		837.9 ± 171.54	
Cortical BMD (mg/cm^3)	Wt	894.07 ± 40.68	4.22×10^{-6}	906.95 ± 122.56	1.2×10^{-3}
	tr/tr	1,125.22 ± 23.74		1,233.55 ± 15.71	
Total bone area (mm^2)	Wt	2.37 ± 0.14	1.11×10^{-4}	2.80 ± 0.29	10.4×10^{-5}
	tr/tr	3.18 ± 0.22		4.00 ± 0.09	
Trabecular bone area (mm^2)	Wt	1.05 ± 0.07	3.04×10^{-4}	1.27 ± 0.13	9.21×10^{-5}
	tr/tr	1.44 ± 0.10		1.80 ± 0.04	
Cortical bone area (mm^2)	Wt	1.31 ± 0.07	9.45×10^{-5}	1.55 ± 0.15	9.48×10^{-5}
	tr/tr	1.77 ± 0.12		2.21 ± 0.05	

Differences between the genotypes were assessed using Student's *t* test ($n = 5$).